

Ionothermal synthesis of octahedral lanthanide–organic coordination networks exhibiting slow magnetization relaxation and efficient photoluminescence

Ting-Hai Yang,^{*a,c} Shu-Fan Wang,^a Chen-Lan Lin,^a Xin Wang,^a Binglong Zhu,^a and Dayu Wu^{*b}

^a*School of Chemistry & Environmental Engineering, Jiangsu University of Technology, Changzhou 213001, P. R. China. E-mail: tinghai_yang@hotmail.com.*

^b*School of petrochemical Engineering, Changzhou University, Changzhou 213164, P. R. China. E-mail: wudy@cczu.edu.cn*

^c*State Key Laboratory of Coordination Chemistry, School of Chemistry & Chemical Engineering, Nanjing University, Nanjing 210093, P. R. China.*

Contents

Scheme S1 Coordination modes of H₂pxdp²⁻ ligand.

Fig. S1 The six-coordinate Dy³⁺ distorted octahedral geometry in **2**.

Fig. S2 The arranged diagram of the two neighbor ligand for **2**.

Fig. S3 Experimental PXRD patterns and simulated ones from single-crystal of **1**.

Fig. S4 TG curves of complexe **1-3**.

Fig. S5 Hysteresis loops in the range of 0-70 kOe for compound **2** at 1.8 K.

Fig. S6 Temperature dependent in-phase (χ_M') and out-of-phase (χ_M'') signals of **2** in zero dc field.

Fig. S7. Frequency dependence of the out-of-phase *ac* susceptibility of **2** at 1.8 K under different external fields.

Fig.S8 Cole–Cole plots for **1** from 1.8 to 13 K under a dc field of 500 Oe.

Fig. S9 The experimental emission quantum yield of **1**.

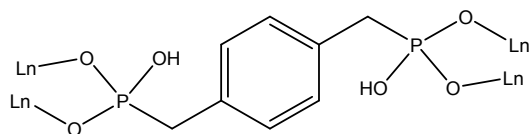
Table S1. Selected bond lengths [Å] for **1-3**.

Table S1. Selected bond angles [°] for **1-3**.

Table S3. Results of the Continuous Shape Measure Analysis geometry

Table S4. Relaxation Fitting Parameters from the Least-Square Fitting of **X** according to the Generalized Debye Model.

Supporting Information



Scheme S1 Coordination modes of $\text{H}_2\text{pxdp}^{2-}$ ligand.

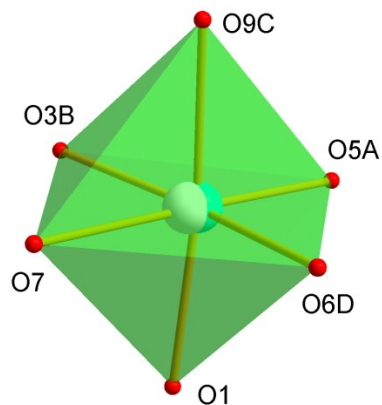


Fig. S1 The six-coordinate Dy^{3+} distorted octahedral geometry in **2**.

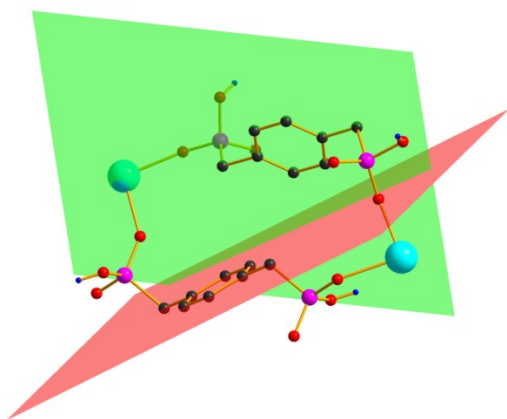


Fig. S2 The arranged diagram of the two neighbor ligand for **2**.

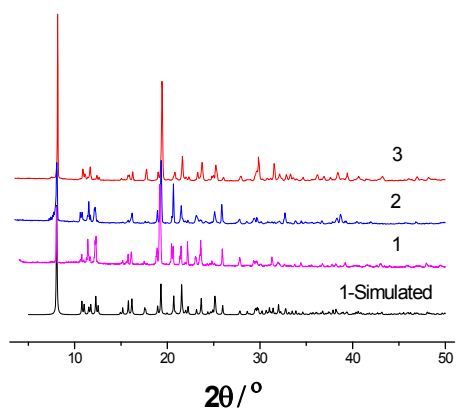


Fig. S3 Experimental PXRD patterns of **1-3** and simulated ones from single-crystal of **1**.

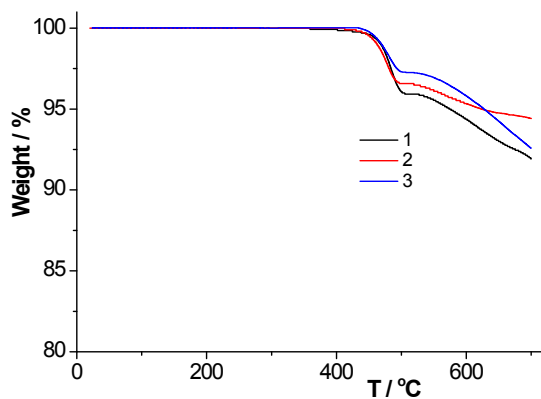


Fig. S4 TG curves of complexe 1-3.

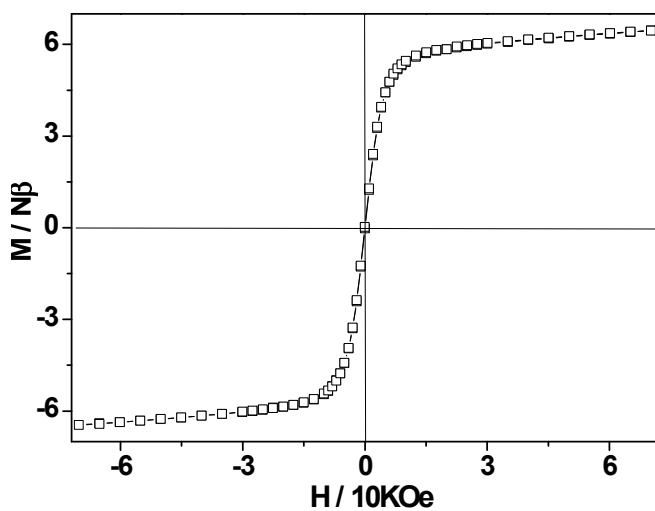


Fig. S5 Hysteresis loops in the range of 0-70 kOe for compound 2 at 1.8 K

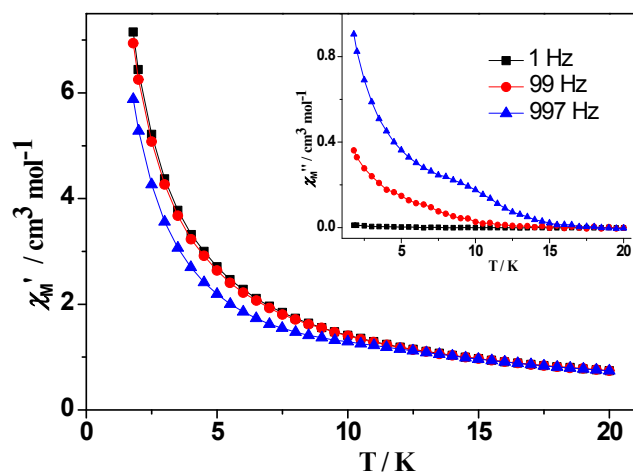


Fig. S6 Temperature dependent in-phase (χ_M') and out-of-phase (χ_M'') signals of 2 in zero dc field.

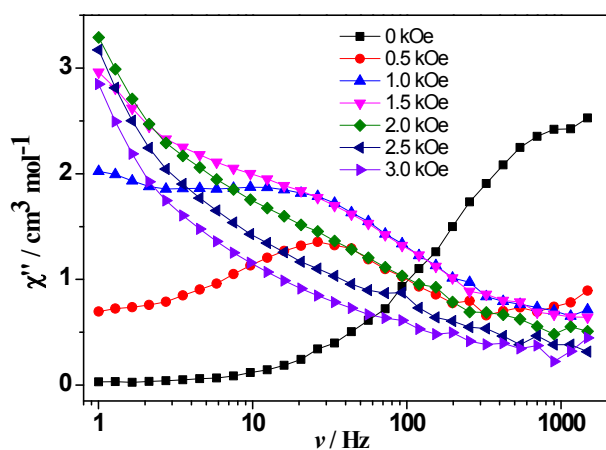


Fig. S7. Frequency dependence of the out-of-phase *ac* susceptibility of **2** at 1.8 K under different external fields.

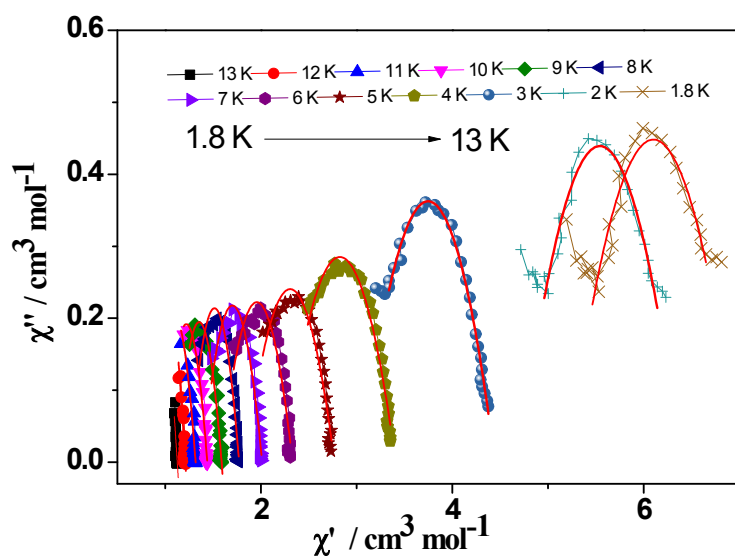


Fig.S8 Cole–Cole plots for **2** from 1.8 to 13 K under a dc field of 500 Oe.

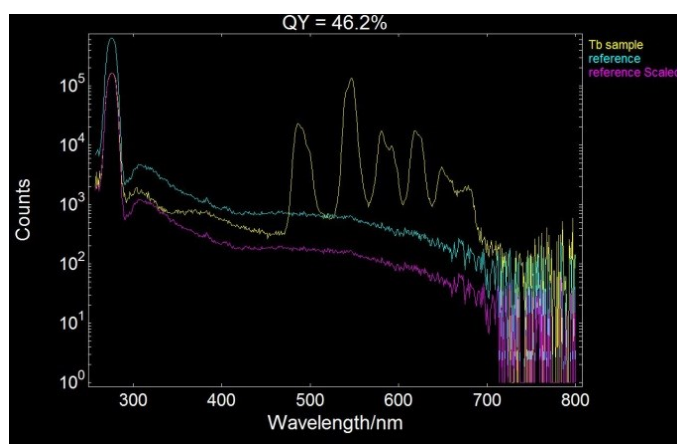


Fig. S9 The experimental emission quantum yield of **1**.

Table S1. Selected bond lengths [Å] for **1-3**.

	1(Tb)	2(Dy)	3(Ho)
Ln(1)-O(5A)	2.213(2)	2.2040(19)	2.1911(14)
Ln(1)-O(1)	2.255(2)	2.2412(18)	2.2365(15)
Ln(1)-O(3B)	2.250(2)	2.2458(18)	2.2321(14)
Ln(1)-O(9C)	2.266(2)	2.2586(19)	2.2457(16)
Ln(1)-O(7)	2.349(2)	2.3351(18)	2.3203(13)
Ln(1)-O(6D)	2.347(2)	2.3358(18)	2.3209(14)
P(1)-O(1)	1.501(3)	1.502(2)	1.5018(16)
P(1)-O(3)	1.506(2)	1.504(2)	1.5091(15)
P(1)-O(2)	1.590(2)	1.595(2)	1.5962(15)
P(1)-C(1)	1.785(3)	1.797(3)	1.794(2)
P(2)-O(5)	1.499(2)	1.4976(19)	1.5007(15)
P(2)-O(6)	1.521(2)	1.522(2)	1.5264(15)
P(2)-O(4)	1.559(3)	1.561(2)	1.5645(17)
P(2)-C(6)	1.785(3)	1.790(3)	1.793(2)
P(3)-O(9)	1.493(3)	1.491(2)	1.4959(17)
P(3)-O(7)	1.519(2)	1.5223(17)	1.5235(14)
P(3)-O(8)	1.564(3)	1.567(2)	1.5715(16)
P(3)-C(9)	1.801(3)	1.794(3)	1.804(2)

Symmerty codes : A: x,y+1,z-1 B: -x+1,-y+2,-z C: -x,-y+2,-z D: -x,-y+2,-z+1

Table S2. Selected bond angles [°] for **1-3**.

	1(Tb)	2(Dy)	3(Ho)
O(5A)-Ln(1)-O(1)	90.36(9)	90.62(8)	90.67(6)
O(5A)-Ln(1)-O(3B)	94.13(9)	94.18(7)	94.31(5)
O(1)-Ln(1)-O(3B)	89.28(9)	89.32(7)	89.43(6)
O(5A)-Ln(1)-O(9C)	95.60(9)	95.38(7)	95.21(6)
O(1)-Ln(1)-O(9C)	173.67(8)	173.72(7)	173.81(5)
O(3B)-Ln(1)-O(9C)	88.16(9)	88.38(7)	88.22(6)
O(5A)-Ln(1)-O(7)	175.60(9)	176.17(7)	176.22(5)
O(1)-Ln(1)-O(7)	86.69(8)	86.71(7)	86.54(5)
O(3B)-Ln(1)-O(7)	82.59(8)	83.06(6)	83.12(5)
O(9C)-Ln(1)-O(7)	87.24(8)	87.21(7)	87.50(5)
O(5A)-Ln(1)-O(6D)	99.80(9)	98.62(7)	98.30(5)
O(1)-Ln(1)-O(6D)	93.90(9)	93.62(7)	93.58(5)
O(3B)-Ln(1)-O(6D)	165.68(8)	166.82(7)	166.99(5)
O(9C)-Ln(1)-O(6D)	87.20(9)	87.33(7)	87.47(6)

Symmerty codes : A: x,y+1,z-1 B: -x+1,-y+2,-z C: -x,-y+2,-z D: -x,-y+2,-z+1

Table S3. Results of the Continuous Shape Measure Analysis geometry^a

Geometry	OC-6	TPR-6	JPPY-6	PPY-6	HP-6
1	0.34	14.889	30.971	27.576	32.960
2	0.28	15.148	31.389	27.951	32.923
3	0.275	15.141	31.373	27.931	32.984

^aOC-6 is the shape measure relative to the octahedron; TPR-6 is the shape measure relative to the trigonal prism; JPPY-6 is the shape measure relative to the Johnson pentagonal pyramid J2; PPY-6 is the shape measure relative to the pentagonal pyramid; HP-6 is the shape measure relative to the Hexagon. The number in bold corresponds to the closer ideal geometry to the real complexes.

Table S4. Relaxation Fitting Parameters from the Least-Square Fitting of **2** according to the Generalized Debye Model under a dc field of 500 Oe.

Temperature / K	$\chi_S / \text{cm}^3\text{mol}^{-1}\text{K}$	$\chi_T / \text{cm}^3\text{mol}^{-1}\text{K}$	τ / s	α
4.0	0.3763	1.524	8.057E-4	0.4202
5.0	0.5026	1.397	7.79464E-4	0.38047
6.0	0.5896	1.310	7.15949E-4	0.30984
7.0	0.6495	1.250	5.62601E-4	0.22368
8.0	0.7443	1.256	3.79416E-4	0.1414
9.0	0.7716	1.228	2.10515E-4	0.12222
10	0.8001	1.200	1.43698E-4	0.06025
11	0.827	1.173	9.32868E-5	0.01764
12	0.760	1.039	7.02876E-5	0.04586